Comparison of the Deuterium Permeability of Copper, CuCrZr, and Cu Layers

A. Houben,[1,*] M. Rasiński,[1] S. Brezinsek,[1] and Ch. Linsmeier[1]

[1] *Forschungszentrum Jülich GmbH, Institut für Energie- und Klimaforschung – Plasmaphysik, Partner of the Trilateral Euregio Cluster (TEC), 52425 Jülich, Germany*

Abstract

In order to estimate the fuel loss in ITER and further future fusion devices, the deuterium permeation through different wall and structural materials are studied. For the obtainment of the effective permeability, gas-driven deuterium permeation measurements are performed on Cu and ITER grade CuCrZr. For a better estimation for fusion reactor components, combined material samples are studied. Cu layers were applied on steel substrates by magnetron sputter deposition. With these studies, the influence of interfaces and microstructure on the hydrogen permeation is investigated. Our study reveal that in the case of Cu layered steel substrates the influence of the interface on the permeation flux is minor compared to the influence of the microstructure on the permeability. The Cu layer permeability is around one order of magnitude smaller than the Cu bulk permeability in the temperature range between 300°C and 550°C.

Keywords:

- gas-driven deuterium permeation
- Cu and Cu layers
- CuCrZr - ITER grade
- microstructure
- interface
- magnetron sputter deposition

CRediT author statement:

- **A. Houben:** Conceptualization, Methodology, Formal analysis, Investigation, Writing - original draft, Visualization, Project administration.
- **M. Rasiński:** Formal analysis, Investigation.
- **S. Brezinsek:** Conceptualization, Resources, Writing - Review & Editing.
- **Ch. Linsmeier:** Conceptualization, Resources, Writing - Review & Editing, Funding acquisition.

I. INTRODUCTION

The estimation of the hydrogen isotopes permeation flux through fusion materials and components is necessary in order to estimate the fuel loss of a fusion device. Furthermore, this knowledge is helpful for the selection of materials and an improved design of components for future fusion devices[1].

Copper, Cu alloys and steels are foreseen as wall materials in ITER and future fusion devices[2,3]. The deuterium permeability of pure Copper and the ITER grade (IG) Cu alloy CuCrZr-IG were measured by gas-driven permeation measurements and are compared to the 316L(N)-IG steel[4].

Since the sample thickness is limited to a few mm, it is not possible to measure a whole component in a gas-driven permeation setup. Therefore, different combinations of fusion materials which will be used in ITER and future fusion devices are under study. Cu layers were deposited by magnetron sputtering on polished 316L(N)-IG substrates. In order to estimate the influence of the interface, three Cu layered substrates were fabricated, characterized and measured with three different Cu layer thicknesses between 490 nm and 1.4 μm. With this, the layer bulk/interface ration was varied in order to separate the influence of the layer microstructure and the influence of the interface on the permeability, see the schematic illustration in Figure 1.

Additional to the measurement of the deuterium permeability through the ITER materials, an overview of different influences on the permeation flux will be obtained by comparison of the permeability of these samples and layered substrates. This knowledge can be used to find out which sample parameters and characteristics are important for a reliable estimation of the permeation flux through a fusion component.

II. SAMPLE PREPARATION

For the pure copper samples, commercial oxygen-free copper was used. The CuCrZr raw material was provided by F4E and the ITER Organization. The CuCrZr blocks were fabricated by Albaksan A.S. and have a composition of about 98.9% Cu, 0.85% Cr and 0.13% Zr according to the test certificate provided by the company. From the raw materials, disks with a diameter of 24 mm and a thickness of 0.5 mm were cut, grinded and polished on

both sides. The last polishing step was with a 1 μm diamond suspension and a cleaning with an oxide polishing suspension was applied afterwards. The polishing procedure was adapted to the hardness of the material in order to obtain a mirror finished surface with no smear layer. The resulting thickness of the substrates after polishing procedure are around 0.3 mm. These samples are named Cu (bulk) and CuCrZr in the following.

For the Cu layered samples, polished 316L(N)-IG samples were used as substrates, please find details to the substrate in [4]. The sample plate of the magnetron device (PREVAC) was rotated during deposition process in order to obtain a homogenous layer. A pure copper sputter target (99.999% Cu, Lesker) was used and an Ar plasma. Several samples were coated during one deposition process, which are identical in microstructure and thickness. The substrates were coated on one side only. The thickness of the layer was varied through the length of the deposition time of each process. Three deposition processes were carried out. The obtained layer thicknesses are 490 nm (named 316L_Cu_thin), 980 nm (named 316L_Cu_thick), and 1400 nm (named 316L_Cu_very_thick). In the following, the terms 'layered substrate' will be used for the complete sample system and 'Cu layer' for the single layer after deduction of the 316L substrate.

Before characterization and measurements, all samples were pre-annealed at the maximum applied temperature of 550°C for several hours in order to remove natural hydrogen and in order to obtain a stable sample condition.

III. MEASUREMENT METHODS

All sample surfaces were analyzed by scanning electron microscopy (SEM) with a Zeiss Crossbeam 540 after pre-annealing. For the Cu layered substrates, cross sections were created by focused ion beam (FIB) enabling a further characterization of the layer by SEM and the measurement of the layer thickness. All figures shown were recorded in SE mode. If needed, energy dispersive X-ray spectroscopy (EDX) measurement was used for elemental analysis. The EDX setup (Oxford X-Max 80) is attached to the SEM(FIB) device.

The gas-driven permeation measurements were performed in an in-house permeation setup. The sample separates two volumes, the low and high pressure volume. Before measurement, both volumes are evacuated to a base pressure of 10^{-9} mbar. After stabilizing the desired

sample temperature, pure deuterium gas is inserted in the high pressure volume and the permeation flux in the low pressure volume is measured by a quadrupole mass spectrometer (Pfeiffer Vacuum). The mass spectrometer is calibrated by four D_2 calibration leaks (LACO Technologies) with fixed deuterium fluxes. The measurement cycles are identical for all samples and the measurement range of the sample temperature is between 300°C and 550°C (up-measurement). At each temperature step, the gas pressure is varied between 25 mbar and 800 mbar. In order to observe a possible change of sample during measurement, after the last temperature step of 550°C, the 500°C to 300°C measurements are repeated (down-measurement). If the up- and down-measurements corresponds to each other, the sample is not change during measurement. The precise thickness of the substrate or the layered substrate are measured by a micrometer screw after permeation measurement in order to avoid scratches on the surface before permeation measurement which could influence the permeation.

IV. DATA ANALYSIS

By measuring the permeation flux deuterium pressure and sample temperature dependent, the process limiting regime and the permeability can be determined. In the diffusion limited regime, where the surface processes are rapid in comparison to the diffusion process, the permeation flux is proportional to the square root of the applied pressure and dependent on the sample or layer thickness. If the permeation flux is linear dependent on the applied pressure, the surface or interface processes limiting the permeation process and the permeation flux is not dependent on the thickness of the sample or layer. In the diffusion limited regime, the permeability constant P_0 and the activation energy E_P can be obtained from the permeation flux J_P:

$$J_P = \frac{P_0\sqrt{p}}{d} e^{\frac{-E_P}{RT}} \tag{1}$$

wherein d is the thickness of the sample, R is the ideal gas constant and T the sample temperature. The obtained permeability $P = P_0 e^{\frac{-E_P}{RT}}$ is valid in the measured temperature and pressure range only.

For the layered substrates, the layer permeability P_{lay} was estimated by the permeability of

the substrate P_{sub} and the permeability of the layered substrate P_{tot}:

$$P_{lay} = \frac{d_{lay}}{\frac{d_{tot}}{P_{tot}} - \frac{d_{sub}}{P_{sub}}} \tag{2}$$

wherein d_{tot}, d_{sub}, and d_{lay} are the thicknesses of the layered substrate, the substrate and the layer, respectively[5]. We want to point out that the layer permeability is an estimation and only valid in the diffusion limited regime, since it scales with the thickness of the layer. It contains all effects which influence the permeability such as surface, interfaces, microstructure and further properties of the layer system. With the layer permeability, a substrate and layer thickness independent value is given with which a comparison of different layers are more reliable.

V. RESULTS

The surface of the polished substrate samples Cu and CuCrZr were analyzed by SEM, see Figure 2. No smear layer of the grinding procedure can be observed and the microstructure is clearly visible. The Cu substrate shows grains of around 50 μm size and voids. The CuCrZr sample shows precipitates with an accumulation around the grain boundaries. An EDX analyzation of this surface confirmed, that the matrix is pure Cu, whereas the precipitates are Cr. A signal from Zr can not be detected by EDX due to the small amount of Zr in the alloy. But the assumption is that the Zr forms CuZr phases[6].

The surface of the Cu layered substrates were analyzed by SEM, see Figure 3 left side. On the right side of Figure 3 the SEM figures of the cross sections through the layers prepared by FIB are shown. The surface structure of the samples 316L_Cu_thin (Fig. 3a) and 316L_Cu_very_thick (Fig. 3c) are similar, whereas the surface of 316L_Cu_thick (Fig. 3b) looks rougher and scratched. In the cross section of the 316L_Cu_thick it is observe that these scratches are on the top of the surface only. The reason for the development of these surface characteristics, which were created during deposition, is unclear, but the influence on the permeation is assumed to be minor. The microstructure of all three layers are similar. The grain size is around two orders of magnitude smaller as in the bulk Cu substrate and no voids, pores, intermediate phases or precipitates can be observed. The layers are homogenous and the thickness was measured on these cross sections: 490 nm (316L_Cu_thin), 980 nm (316L_Cu_thick), and 1400 nm (316L_Cu_very_thick).

Sample	p^x	P_0 $\left[\frac{\text{mol}}{\text{ms}\sqrt{\text{mbar}}}\right]$	E_P $\left[\frac{\text{kJ}}{\text{mol}}\right]$
Cu	0.55	$3(2)\cdot10^{-6}$	77(2)
CuCrZr	0.55	$6(2)\cdot10^{-6}$	79(1)
316L_Cu_thin	0.6	$4(2)\cdot10^{-7}$	55(2)
316L_Cu_thick	0.6	$2.3(5)\cdot10^{-6}$	66(2)
316L_Cu_very_thick	0.65	$1.3(5)\cdot10^{-6}$	63(2)
316L[4]	0.5	$8(1)\cdot10^{-7}$	58(1)

TABLE I. The results obtained from temperature and pressure dependent permeation measurements: pressure dependence p^x, permeation constant P_0, and activation energy E_P. The values for the 316L substrate are taken from [4].

As an example, the permeation flux versus the applied deuterium pressure and the Arrhenius plot are shown for the 316L_Cu_thick sample in Figure 4. From Figure 4a the pressure dependence was extracted for each temperature step and a mean value is given in Table I. The permeability was obtained from the Arrhenius plot (Figure 4b) for each pressure step, and the mean values for the permeation constant P_0 and the activation energy E_P is given in Table I. The same analyzation was performed on each sample and summarized in Table I. The given values are valid in the measured temperature (300°C to 550°C) and pressure (25 mbar to 800 mbar) range. Since the up- and down-measurements corresponds to each other, no change of sample during measurement is observed. The data for the 316L substrate were taken from the publication [4] and will be used for the calculation of the Cu layer permeability. The permeabilities versus sample temperature of all samples listed in Table I are shown in Figure 5.

The layer permeabilities of all Cu layers are calculated according to Equation 2. For the substrate permeability, the values for 316L was used. For the layered substrate permeability, the values for 316L_Cu_thin, 316L_Cu_thick, and 316L_Cu_very_thick are taken from Table I. The layer permeabilities can be found in Table II and are plotted in Figure 6.

Layer	P_0 $\left[\frac{\text{mol}}{\text{ms}\sqrt{\text{mbar}}}\right]$	E_P $\left[\frac{\text{kJ}}{\text{mol}}\right]$
Cu_thin Layer	$3{\cdot}10^{-10}$	42
Cu_thick Layer	$2{\cdot}10^{-6}$	93
Cu_very_thick Layer	$3{\cdot}10^{-7}$	80
MV Cu Layer	$7{\cdot}10^{-8}$	72

TABLE II. The layer permeabilities estimated according to Equation 2. The mean value (MV) of the Cu layers are calculated from the permeabilites of the three Cu layer pemerabilites, see text.

VI. DISCUSSION

The permeabilites of the Cu and the CuCrZr samples are very similar and P_0 and E_P of CuCrZr are within the error bars of the values for Cu. From this it is concluded that the precipitates does not influences the permeability and that the permeability is mainly defined by the Cu matrix. In both cases, the diffusion is limiting the permeation process, as expected for polished samples. The measured value for the Cu sample are in agreement to the adapted literature value for deuterium permeation through Copper[7].

In the Cu layered substrates the permeation process is mainly limited through the diffusion process, see Table I. A reduction of the permeability of the 316L_Cu samples is expected due to the coating in comparison to the uncoated substrate, because Cu shows a lower permeability than 316L. The expected permeability of the 316L_Cu_very_thick sample was calculated with Equation 2 by using the permeabilities of Cu bulk and 316L from Table I. The result is shown in black dotted lines in Figure 5. The expected reduction is very small. Comparing the expected permeability with the measured permeability of the 316L_Cu_very_thick sample, the measured permeability is lower as expected. By calculating the Cu layer permeability the difference can be seen in Figure 6. The permeability of the Cu layer is about one order of magnitude lower as the bulk Cu permeability.

As explained above, the layer permeability contains all sample characteristics, such as effects of interfaces, microstructure and surface effects. In order to study if the interface is the reason for the reduced Cu layer permeability or any other effect, the layer thickness was varied as explained above and illustrated in Figure 1: The Cu layer permeability contains

the permeability of the layer bulk (P_{LB}) and the interface (P_{int}). By varying the layer thickness, the layer bulk and interface ratio was varied and the influence of the interface and the bulk (microstructure) can be separated. If the microstructure is the reason for the difference compared to the Cu bulk sample, the permeability of the Cu layer would be diffusion limited and therefore scale with the thickness of the layer. Furthermore, Equation 2 would be valid and the layer permeability of all Cu layers would be the same. In the opposite case, in which the influence of the interface plays the major role for the difference, the layered substrate permeability should be very similar in all layered substrates and independent on the layer thicknesses. Equation 2 would not be valid which would lead to an increase of the calculated layer permeability with increasing the layer thickness.

In the layered substrate permeability in Figure 5 and Table I no clear behavior can be extracted. There is a difference between all layered substrate permeabilities and since the P_0 and E_P are very different, the slope of the curves are different as well. The differences in slope can be observed in the layer permeabilities as well, see Figure 6 and Table II. Nevertheless, since the layer permeabilities are all in the same order of magnitude, the assumption is that the microstructure is the major reason for the larger reduction of the layer permeability compared to the Cu bulk sample. Since the pressure dependence is only slightly increased in the layered substrates, see Table I, the diffusion is mainly limiting the permeation process. This is another indication that the interface do not have a significant influence on the permeation flux in this case.

A mean value (MV) was calculated from all three Cu layer permeabilites, see Table II and the brown curve in Figure 6. From this Cu Layer MV the layered substrate permeability was calculated for the 316L_Cu_very_thick sample, see black line in Figure 7. As a summary, a comparison is shown in this figure between the Cu bulk, the Cu layer MV, the calculated 316L_Cu_very_thick sample with the Cu bulk value (black dotted line) and the measured 316L_Cu_very_thick sample permeability. The conclusion is that there might be an influence of the interface on the permeation, but in this case the influence of the microstructure on the permeation is much larger and the major reason for the reduction.

VII. CONCLUSIONS

In both polished Cu and CuCrZr samples, diffusion is limiting the permeation process. The permeabilities of Cu and CuCrZr are similar and in agreement with literature data for Cu.

The measured reduction of the 316L permeability due to the Cu coating is much larger as expected from an estimation using the Cu bulk permeability. By varying the layer thickness, the layer bulk and interface ratio was changed and the influence on the permeability of the microstructure and the interface could be separated. The conclusion is, that the influence of the microstructure is the major reason for the reduction and the influence of the interface on the permeability is minor is this case. The Cu layer permeability is about one order of magnitude smaller as the Cu bulk permeability. Further material combinations, e.g., W on CuCrZr, are under study.

ACKNOWLEDGEMENTS

The authors thank G. De Temmerman (ITER Oranisation) and S. Heikkinen (F4E) for providing the CuCrZr-IG sample material and B. Göths for sample preparation.

This work has been carried out within the framework of the EUROfusion Consortium, funded by the European Union via the Euratom Research and Training Programme (Grant Agreement No 101052200 — EUROfusion and 2019-2020 under grant agreement No 633053). Views and opinions expressed are however those of the author(s) only and do not necessarily reflect those of the European Union or the European Commission. Neither the European Union nor the European Commission can be held responsible for them.

---

* an.houben@fz-juelich.de

[1] R. Causey, JOURNAL OF NUCLEAR MATERIALS **300**, 91 (2002).

[2] K. Ioki, P. Barabaschi, V. Barabash, S. Chiocchio, W. Daenner, F. Elio, M. Enoeda, A. Gervash, C. Ibbott, L. Jones, V. Krylov, T. Kuroda, P. Lorenzetto, E. Martin, I. Mazul, M. Merola, M. Nakahira, V. Rozov, Y. Strebkov, S. Suzuki, V. Tanchuk, R. Tivey, Y. Utin, and M. Yamada, NUCLEAR FUSION **43**, 268 (2003).

[3] M. Li and S. J. Zinkle, in *COMPREHENSIVE NUCLEAR MATERIALS, VOL 4: RADIATION EFFECTS IN STRUCTURAL AND FUNCTIONAL MATERIALS FOR FISSION AND FUSION REACTORS*, edited by R. Konings (2012) pp. 667–690.

[4] A. Houben, J. Engels, M. Rasiński, and C. Linsmeier, Nuclear Materials and Energy **19**, 55 (2019).

[5] A. Houben, M. Rasinski, and C. Linsmeier, PLASMA AND FUSION RESEARCH **15** (2020), 10.1585/pfr.15.2405016.

[6] P. Ostachowski, W. Bochniak, M. Lagoda, and S. Ziolkiewicz, INTERNATIONAL JOURNAL OF ADVANCED MANUFACTURING TECHNOLOGY **105**, 5023 (2019).

[7] R. Causey, R. Karnesky, and C. S. Marchi, in *Comprehensive Nuclear Materials*, edited by R. J. Konings (Elsevier, Oxford, 2012) pp. 511 – 549.

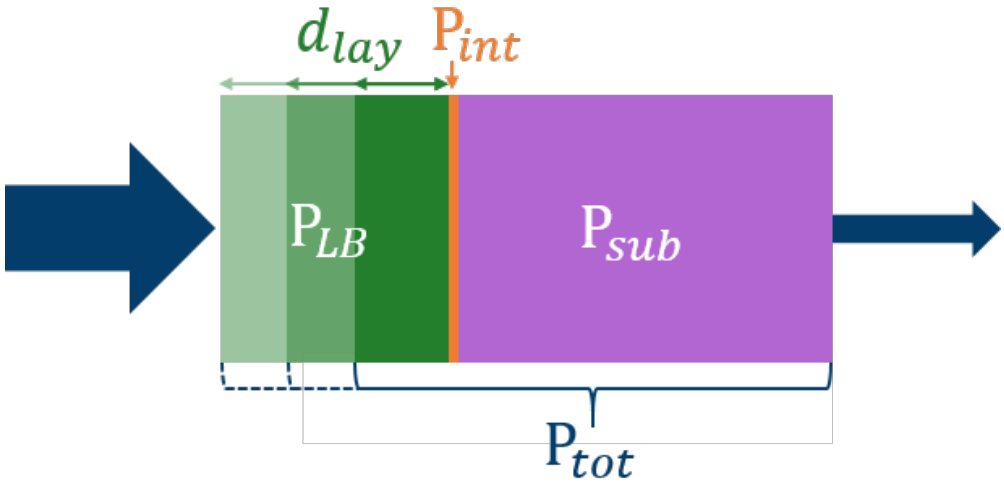

FIG. 1. Schematic illustration of the layer thickness variation. d_{lay} represents the layer thickness, P_{tot}, P_{sub}, P_{LB}, and P_{int} the permeability of the layered substrate, the substrate, the layer bulk, and the interface, respectively. The shown proportions do not correspond to the real thicknesses and are for illustration only.

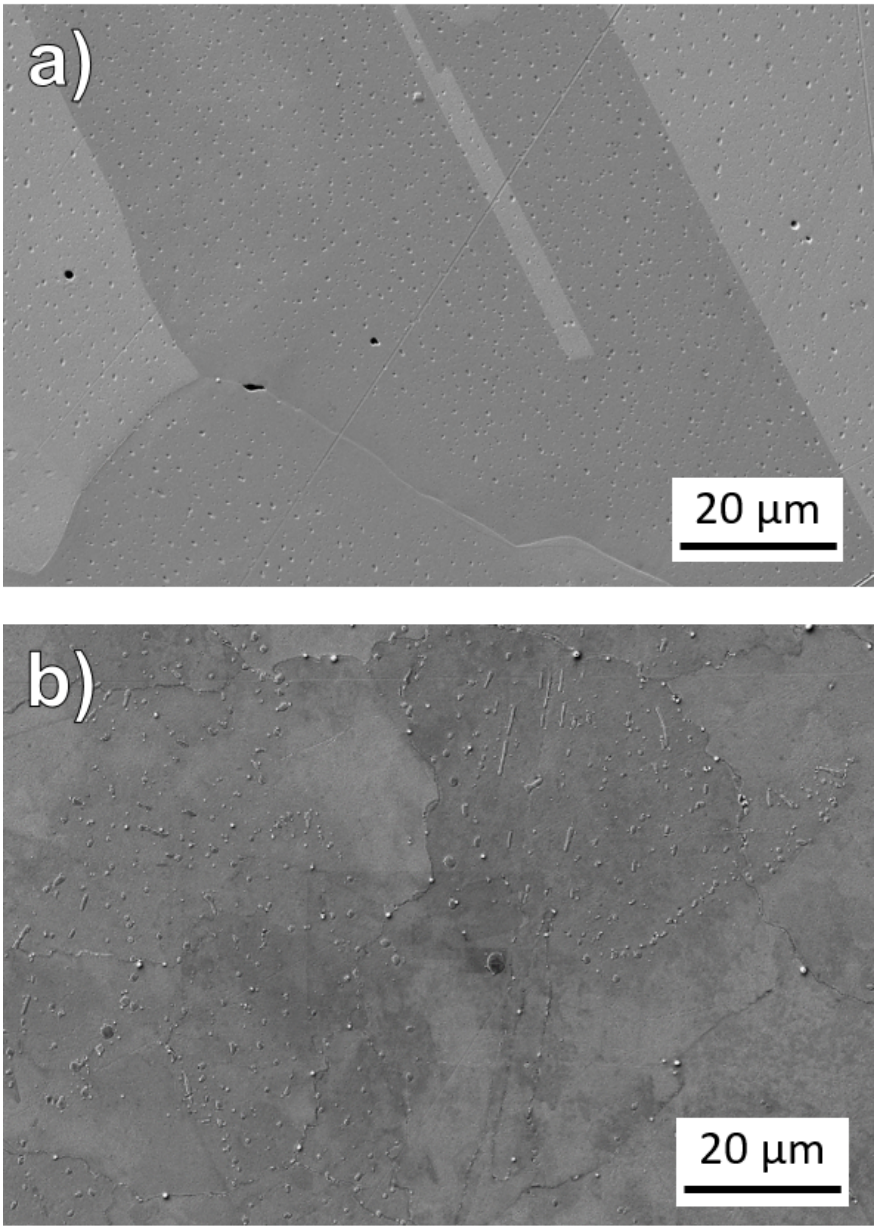

FIG. 2. SEM figures of the polished surfaces: a) Cu b) CuCrZr.

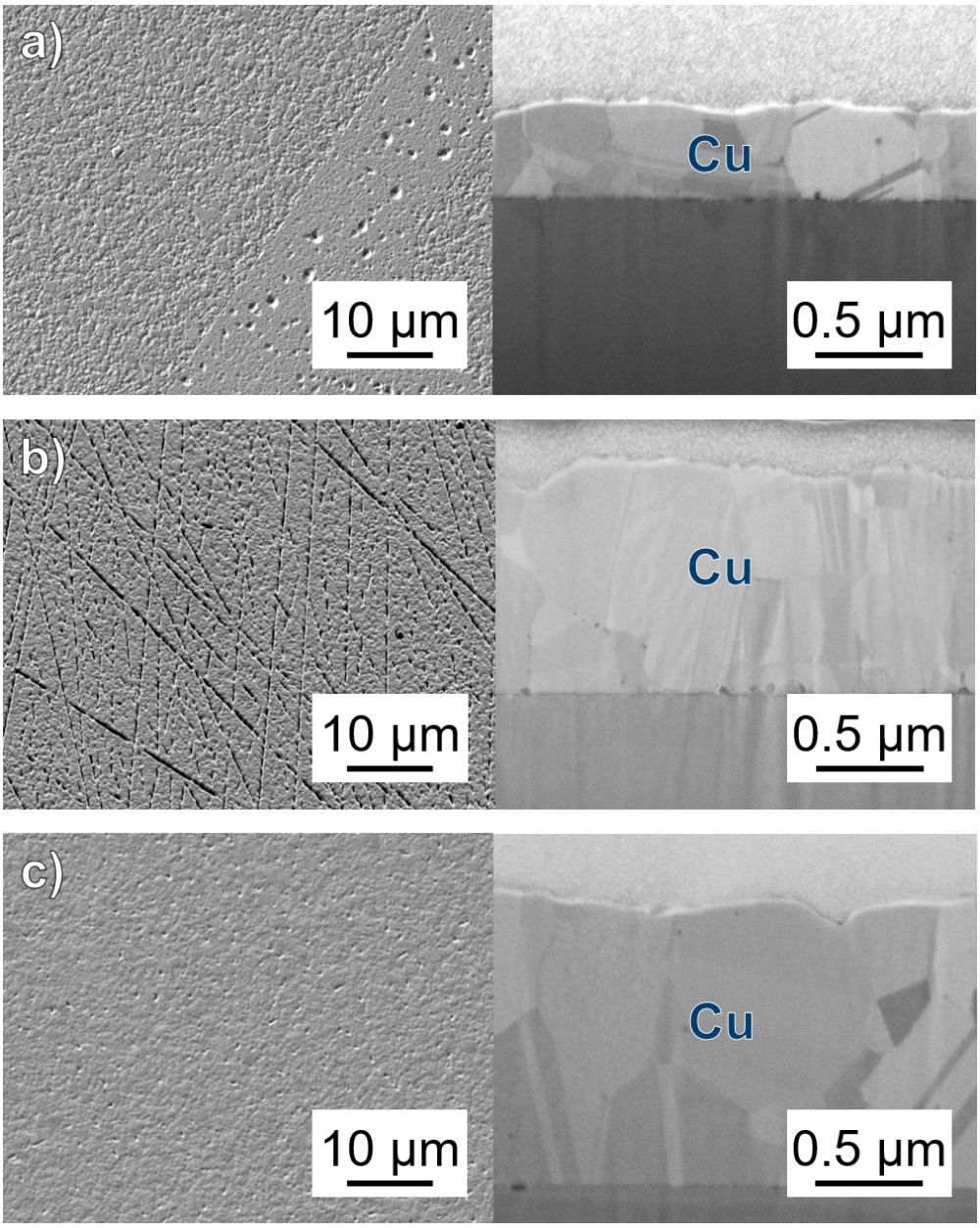

FIG. 3. Left: SEM figures of the surface; Right: SEM figures on the cross sections prepared by FIB of the coated substrates: a) 316L_Cu_thin; b) 316L_Cu_thick; c) 316L_Cu_very_thick. On top of the Cu layer, a Pd layer is visible. The Pd layer was applied for the FIB cut in order to avoid surface damage and the curtaining effect during FIB cut.

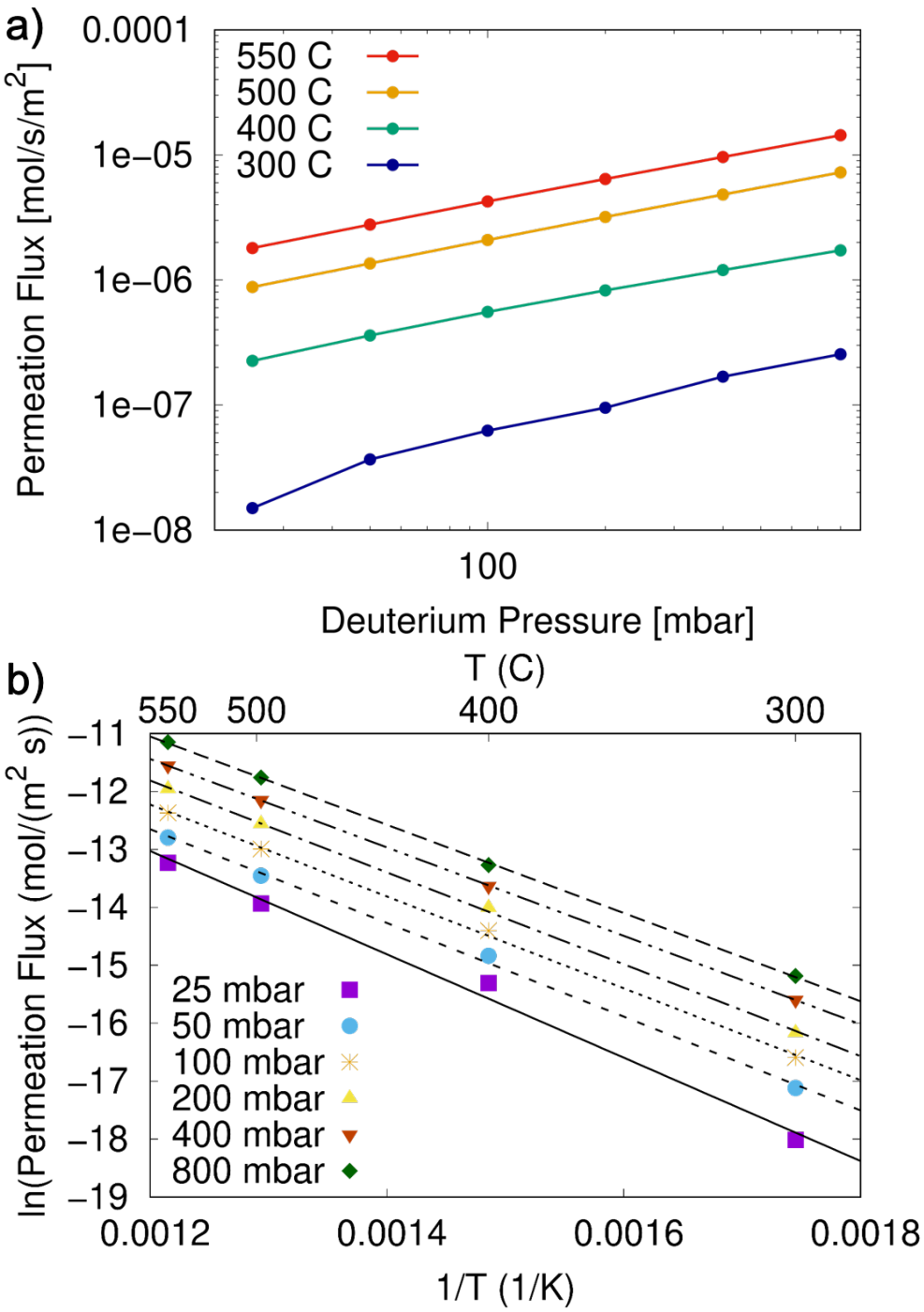

FIG. 4. a) Stabilized permeation flux through the 316L_Cu_thick sample versus the applied deuterium pressure. The colors indicate the sample temperatures. b) The corresponding Arrhenius plot for the 316L_Cu_thick sample. The lines represent the fitted lines to the data in order to obtain E_P and P_0, see Table I. The color points represent the measurement points at different applied deuterium pressures.

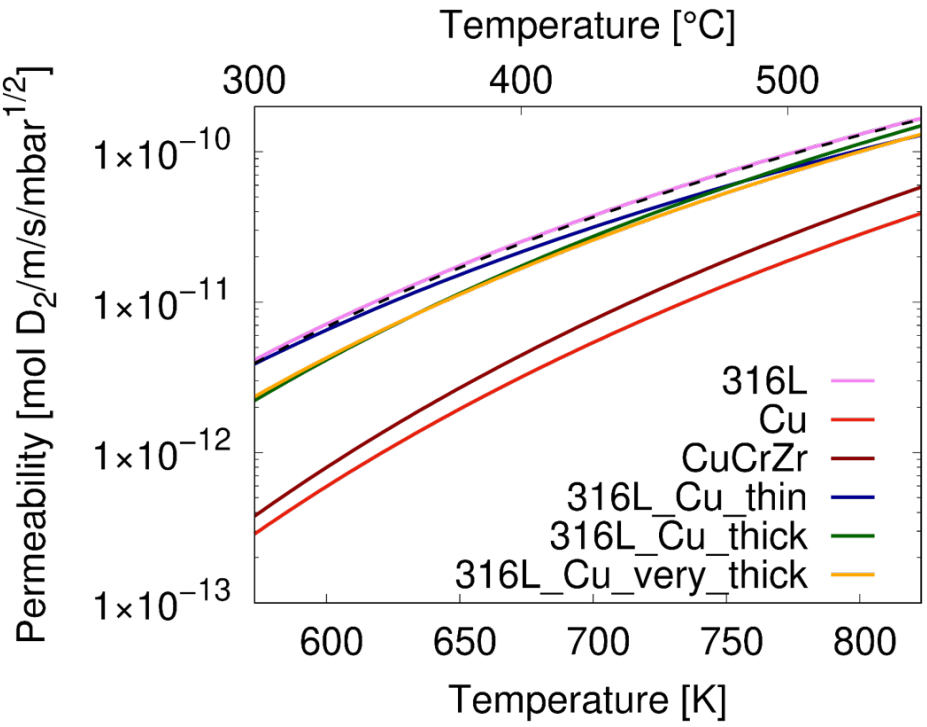

FIG. 5. Permeability versus sample temperature for Cu, CuCrZr and the Cu layered 316L substrates with the values from Table I. The permeability for the 316L substrate is taken from [4]. The black dotted line is the estimated permeability for the 316L_Cu_very_thick sample by using the Cu bulk value, see text.

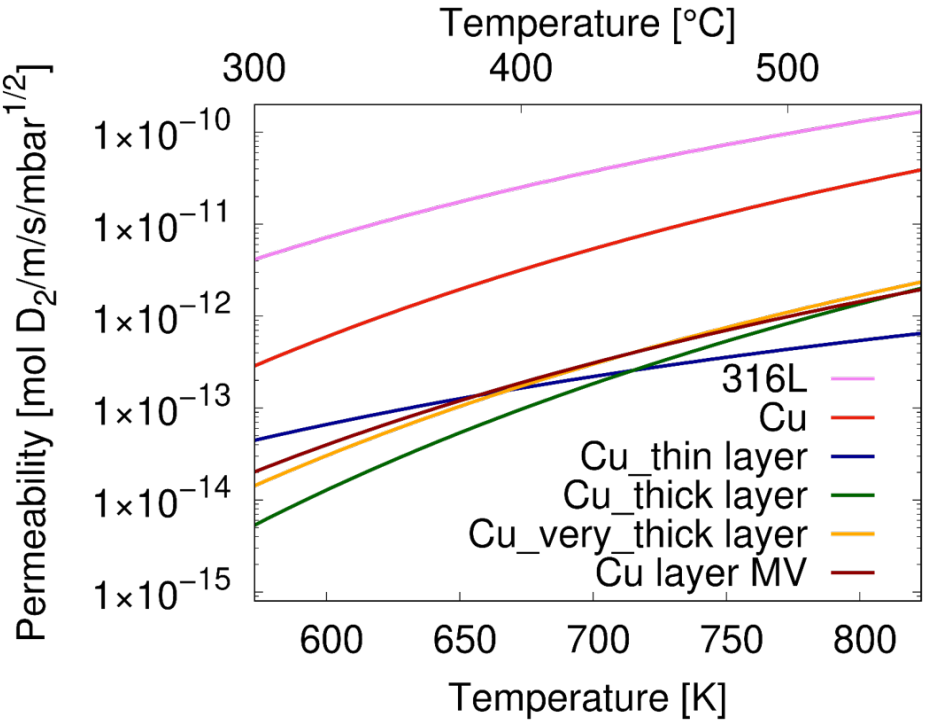

FIG. 6. Permeability versus sample temperature for the Cu layers from Table II and for comparison of the bulk Cu and 316L substrates. The mean value (MV) of the Cu layers are calculated from the permeabilites of the three Cu layer pemerabilites, see text.

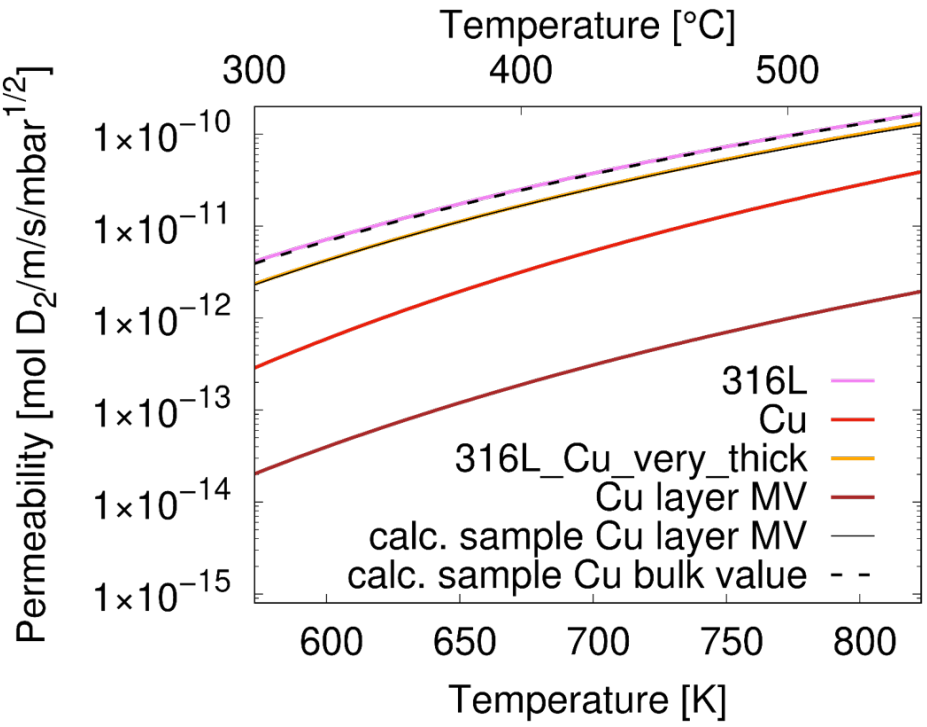

FIG. 7. The 316L_Cu_very_thick sample permeability (black line) calculated with the Cu Layer MV (brown line). For comparison, the Cu bulk, the calculated 316L_Cu_very_thick sample with the Cu bulk value, and the measured 316L_Cu_very_thick sample permeabilities are shown.